EFFECT OF GADOLINIUM CONTENT ON MAGNETIC AND STRUCTURAL CHARACTERISTICS OF NFGO NANO-PARTICLES

Sara Durga Bhavani[a,e], K. Vijaya Kumar[b]*, A.T. Raghavender[c], J. Arout Chelvane[d], B. Purna Chandra Rao[e]*

[a] *Department of Chemistry, Government Degree College Rajendranagar, Rangareddy District - 501218, Telangana, India*
[b] *Department of Physics, JNTUH University College of Engineering Jagtial, Nachupally (Kondagattu), Jagtial District 505501, Telangana, India*
[c] *Department of Physics, International School of Technology and Sciences for Women, Rajamahendravaram, East Godavari - 533 294, Andhra Pradesh, India*
[d] *Advanced Magnetic Group, Defence Metallurgical Research Laboratory, Kanchanbagh, Hyderabad-500 058, Telangana, India*
[e] *Department of Chemistry, Gandhi Institute of Technology and Management, Hyderabad-502 329, Telangana, India*
*Corresponding Author e-mail: kvkphd@gmail.com; pbhavnar@gitam.edu

Sol gel auto-combustion was used to create gadolinium doped nickel ferrite nano-particles, which have chemical composition $NiFe_{2-x}Gd_xO_4$ (x = 0.00, 0.010, 0.15, 0.20 & 0.25). The investigation focused on how the composition of Gd^{+3} affected the magnetic properties and structural parameters. Magnetic properties were investigated using VSM technique, structural properties were determined using XRD and SEM techniques. XRD graphs verified the establishment of the spinel ferrite phase. With an increase in Gd composition, the crystallite size and lattice parameter increased from 21.0288 to 27.04125 nm and 8.3325 to 8.3367Å, respectively. It was also evident how the composition of Gd^{+3} affected the estimation of bond-angles and lengths in tetrahedral and octahedral structures. SEM micrographs showed that all of the grains had a small amount of agglomeration and that all of the synthesized compositions were homogenous. The range of 140.5–176.2 nm was found to be the average grain size. Using VSM at 300K, magnetic parameters like coercivity, residual magnetization, and saturation magnetization were computed. Until the composition was 0.20, the saturation magnetization and residual magnetization dropped from 30.28 emu/g to 15.35 emu/g and 5.07 emu/g to 3.65 emu/g, respectively. After that, they increased to 34.40 emu/g and 6.52 emu/g, respectively. Until composition 0.20, coercivity was raised from 154 to 261 Oe; after that, it was lowered to 233 Oe.
Keywords: *Gadolinium doped nickel ferrite nano-particles; Sol gel auto-combustion; XRD; SEM and magnetic properties*
PACS: 75.50.Gg, 61.05.cp, 61.05.cp, 68.37.Hk, 75.75.Fk

INTRODUCTION

The applications of spinel ferrite nano-particles in current context include drug delivery, photocatalysis, telecommunications, electronics, and electrical devices like transformer cores, permanent magnets, magnetic refrigeration, magnetic recording media, gas sensors, and microwave absorbers, among others [1-5]. Spinel ferrite is generally represented by the formula AB_2O_4, where the B-site is referred to as octahedral at the center of the octahedron and the A-site is referred to as tetrahedral since it is positioned at the center of the tetrahedron and contains oxygen-ions at each corner. The big oxygen-ions are arranged in a face-cantered cubic configuration with space between them occupied by metal-ions [6-7]. The inverse spinel structure of nickel ferrite, one of the ferrites that has been the subject of extensive research as a magnetic nanomaterial, shows that trivalent Fe^{+3} ions occupy both [A] and [B] sites whereas divalent Ni^{+2} ions occupy the octahedral [B] sites [8-9]. Researchers have employed a variety of methods to analyze the structural; electrical; optical; and magnetic properties; of their ferrite nano-particles in order to determine the impact of doping elements and manufacturing methods [10–12]. Their characteristics can be changed by doping them with rare earth elements in a cubic spinel ferrite structure [13-14]. Due to its half-filled $4f^7$ electronic configuration, gadolinium is a magnetically active high spin rare earth metal. The properties of the ferrites can be affected by a small amount of Gd doping. Since rare earth ions have high spin-orbit coupling and unpaired (4f) electrons, it is known that Fe-Fe exchanges in ferrites are caused by the spin coupling of (3d) electrons, which affects the structural, electrical, optical, and magnetic properties. Better magnetic and electrical properties result from rare earth ion interaction with Fe, or 3d–4f coupling, when these ions occupy ferrite lattice positions [15–16]. Furthermore, studies on the doping of ions in $CoFe_2O_4$ nano-particles have been published, and the results indicate that the characteristics of ferrites vary significantly [13]. There are few studies on Gd-doped nickel ferrites nano-particles in the literature that has been released [17–18], with the exception of those that concentrate on the composite materials' magnetic characteristics. Consequently, the composition of Gd^{+3} affects structural characteristics and magnetic properties in the current work, which is synthesized using the Sol gel (auto-combustion) process.

II. EXPERIMENTAL

According to Figure.1 [19–21], sol gel (auto-combustion) process was used to create $NiFe_{2-x}Gd_xO_4$ (x = 0.00, 0.010, 0.15, 0.20 & 0.25) ferrite nano-particles.

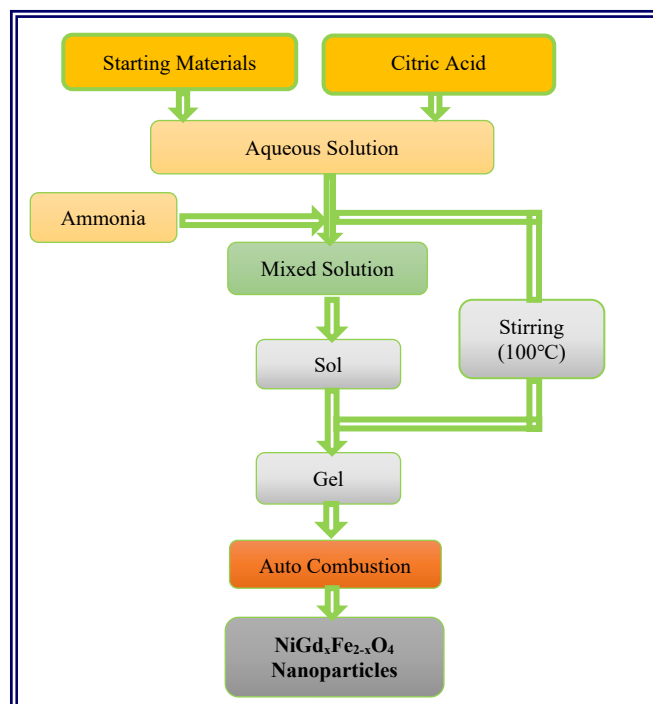**Figure 1.** Flowchart of synthesis of NiFe$_{2-x}$Gd$_x$O$_4$ (x = 0.00, 0.05, 0.10, 0.15, 0.20 & 0.25) ferrite nano-particles

The precursor materials included ammonia, citric acid, ferric and gadolinium nitrates were AR graded. De-ionized water was used to dissolve the precursor materials in a stoichiometric ratio to create a transparent solution. The solution containing Ni^{+2}, Gd^{+3}, and Fe^{+3} ions was chelated by adding citric acid to the organized aqueous solution. Citric acid and total moles of nitrate ions were combined in 1:3 molar ratio. The attained solution was neutralized with ammonia in an appropriate amount to maintain a p^H of 7. A hot plate was then used to heat the neutralized solution to approximately 100℃ while stirring continuously. A thick gel was seen a few hours later. A loose powder [22–23] remained after the temperature was raised to 200℃, which started the ignition process and caused the generated gel to burn completely through auto-combustion. It was annealed for eight hours at 700 ℃ and was known as "as-prepared powder."

Using a Phillips expert X-ray diffractometer, the XRD patterns for NiFe$_{2-x}$Gd$_x$O$_4$ (x = 0.00, 0.010, 0.15, 0.20 & 0.25) ferrite nano-particles were obtained. The NiFe$_{2-x}$Gd$_x$O$_4$ (x=0.00, 0.010, 0.15, 0.20 & 0.25) ferrite nano-particles' microstructural morphology was examined using a ZEISS EVO-18 SEM. VSM were used to measure the magnetic properties at 300 K and a maximum applied magnetic field (15 kOe).

RESULTS AND DISCUSSIONS

Figure 2 displays XRD patterns of NiFe$_{2-x}$Gd$_x$O$_4$ (x = 0.00, 0.10, 0.15, 0.20, 0.25) ferrite nano-particles that were annealed for eight hours at 700℃ [25]. Single-phase; cubic spinel structure; and Fd3m space-group; are indicated by XRD patterns. Because of nano-crystalline pattern of the prepared compositions, XRD data showed that XRD peaks grew wider with increasing Gd doping content. The variance in ionic-radius of Ni (0.74 Å) and Gd (0.94 Å) could be cause of slight shift in peak position observed with increase in Gd^{+3} composition. Various structural parameters were computed from XRD patterns using standard relations listed below.
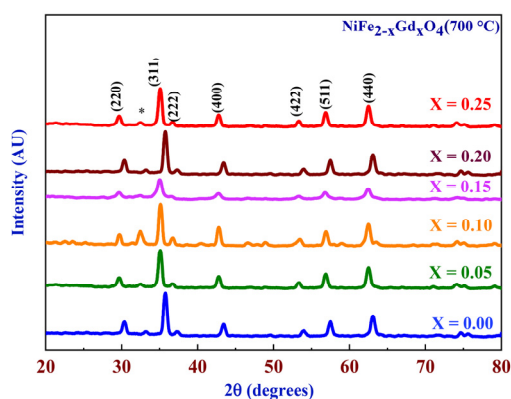

Figure 2. XRD pattern of NiFe$_{2-x}$Gd$_x$O$_4$ (x = 0.00, 0.05, 0.10, 0.15, 0.20 & 0.25) ferrite nano-particles annealed at 700℃
[K.V. Kumar et al, (2023), Eur. Chem. Bull. 2023,12(4) 10479-1048]

The crystallite-size (D) of $NiFe_{2-x}Gd_xO_4$ (x = 0.00, 0.010, 0.15, 0.20 & 0.25) ferrite nano-particles was calculated for present XRD patterns using the Scherrer's formula [25]:

$$D = \frac{0.94\lambda}{\beta \cos\theta} \tag{1}$$

where, θ -diffraction angle, λ-wavelength (Co Kα radiation), β-FWHM and D-crystallite size.

Using 2θ-values, interplanar spacing & lattice parameter of $NiFe_{2-x}Gd_xO_4$ (x= 0.00, 0.010, 0.15, 0.20 & 0.25) ferrite nano-particles was calculated with the following formula [26]:

$$a = \frac{d}{\sqrt{h^2+k^2+l^2}} \tag{2}$$

Crystallite size and lattice parameter were observed to increase with Gd^{+3} composition and were obtained in the range of 21.0288 to 27.04125 nm and 8.3325 to 8.3367Å respectively are tabulated in Table 1 and shown their variation with Gd composition in Figure 3. The improved values of lattice parameter confirmed the entrance of Gd^{+3} ions into the structure [27-28].

Table 1. Average Crystallite size, Lattice parameter and average interplanar spacing & average grain size of $NiFe_{2-x}Gd_xO_4$ (x = 0.00, 0.05, 0.10, 0.15, 0.20 & 0.25) ferrite nano-particles annealed at 700℃.

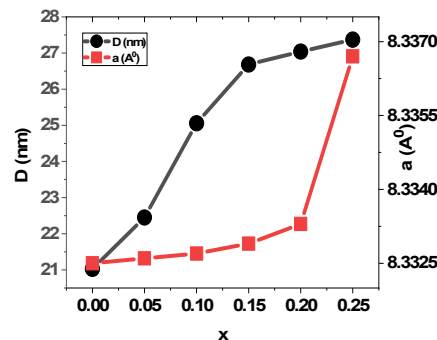| Gd Composition	Average Crystallite Size (nm)	Lattice parameter (Å)	Average Interplanar spacing (Å)	Average Grain size (nm)
0.0	21.02875	8.3325	2.17625	140.5
0.05	22.45000	8.3326	2.20625	145
0.10	25.06000	8.3327	2.20625	159.1
0.15	26.68375	8.3329	2.20500	153.33
0.20	27.04125	8.3333	2.20750	154.2
0.25	27.37250	8.3367	2.18875	176.2

Figure 3. Variation of crystallite size (D) and lattice constant (a) for $NiFe_{2-x}Gd_xO_4$ (x = 0.00, 0.05, 0.10, 0.15, 0.20 & 0.25) ferrite nano-particles annealed at 700℃

Three different kinds of magnetic-interactions between the cations could be possible via intermediate oxygen-ions through the super-exchange mechanism because the metal-ions occupy at two different lattice sites in the spinel structure: A-A interaction, B-B interaction, and A-B interaction. The angles between cations dispersed over two sites and the distances between cations and oxygen determine an amount of interaction energy between relating cations. In order to investigate how the composition of Gd^{+3} affected the structural characteristics of the ferrite nanoparticles, as illustrated in Figure 4 [29].
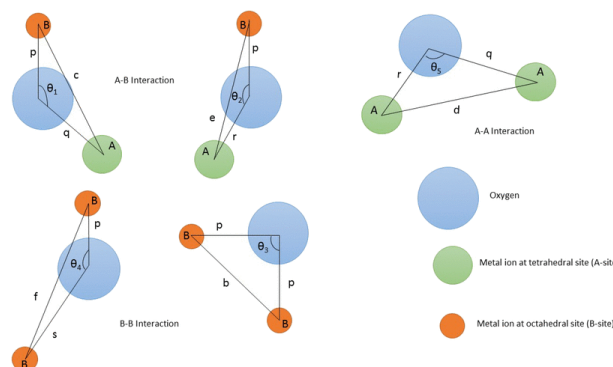

Figure 4. Ion pair configuration in spinel ferrite with bond lengths and bond angles [Raghvendra Singh Yadav et al., 2018, Journal of Materials Science: Materials in Electronics, 29, 15878-15893]

The bond-lengths between the cations at the tetrahedral and octahedral sites designated as b, c, d, e, and f were estimated. The subsequent formulas (3–7) [30] can be used to assess these:

$$b = \sqrt{2}\left(\frac{a}{4}\right) \tag{3}$$

$$c = \sqrt{11}\left(\frac{a}{8}\right) \tag{4}$$

$$d = \sqrt{3}\left(\frac{a}{4}\right) \tag{5}$$

$$e = \sqrt{3}\left(\frac{3a}{8}\right) \tag{6}$$

$$f = \sqrt{6}\left(\frac{a}{4}\right) \tag{7}$$

The bond lengths of the ferrite nano-particles between metal-ions and oxygen at various sites are denoted by the following equations (8-11) [30] and are represented as p, q, r, and s (bond-lengths between cation-anion) in Figure-4 [29]:

$$p = a\left(\frac{5}{8} - u\right) \tag{8}$$

$$q = a\sqrt{3}\left(u - \frac{1}{4}\right) \tag{9}$$

$$r = a\sqrt{11}\left(u - \frac{1}{8}\right) \tag{10}$$

$$s = a\sqrt{3}\left(\frac{u}{3} + \frac{1}{8}\right) \tag{11}$$

Equations (12-16) [31] can be used to determine the bond-angles between cations (oxygen-ions) and cation-anion (metal-ions) of the ferrite nano-particles, which are represented as θ_1, θ_2, θ_3, θ_4 and θ_5. The same was depicted in Figure-4 [28]:

$$\theta_1 = \cos^{-1}\left(\frac{p^2+q^2-c^2}{2pq}\right) \tag{12}$$

$$\theta_2 = \cos^{-1}\left(\frac{p^2+r^2-e^2}{2pr}\right) \tag{13}$$

$$\theta_3 = \cos^{-1}\left(\frac{2p^2-b^2}{2p^2}\right) \tag{14}$$

$$\theta_4 = \cos^{-1}\left(\frac{p^2+s^2-f^2}{2ps}\right) \tag{15}$$

$$\theta_5 = \cos^{-1}\left(\frac{p^2+q^2-d^2}{2rq}\right) \tag{16}$$

Tables 2, 3 & 4 contains a tabulation of all bond-length values and bond-angle values between cations and cation-anions. It was discovered that the Gd^{+3} composition increased the interatomic distance between the cations at two distinct sites (A & B) and the cation-anion. The greater ionic radius of Gd^{+3} ions is the cause of this variation. A-B and B-B interactions were found strengthened, as indicated by the increased bond-angles θ_1, θ_2, θ_3, θ_4 and θ_5 [32–33].

Table 2. Variation of bond lengths between cations situated in $NiFe_{2-x}Gd_xO_4$ (x = 0.00, 0.05, 0.10, 0.15, 0.20 & 0.25) ferrite nano-particles annealed at 700°C

Gd Composition	b (Å)	c (Å)	d (Å)	e (Å)	f (Å)
0.0	2.945984	3.454472	3.608078	5.412118	5.102593
0.05	2.946019	3.454513	3.608122	5.412182	5.102655
0.10	2.946054	3.454555	3.608165	5.412247	5.102716
0.15	2.946125	3.454638	3.608252	5.412377	5.102838
0.20	2.946266	3.454804	3.608425	5.412637	5.103083
0.25	2.947469	3.456213	3.609897	5.414845	5.105165

Table 3. Variation of bond lengths between cation-anion situated in $NiFe_{2-x}Gd_xO_4$ (x=0.00, 0.05, 0.10, 0.15, 0.20 & 0.25) ferrite nano-particles annealed at 700°C

Gd Composition	p (Å)	q (Å)	r (Å)	s (Å)
0.0	2.083125	1.804039	6.908944	3.6080783
0.05	2.08315	1.804061	6.9090269	3.6081216
0.10	2.083175	1.804082	6.9091098	3.6081649
0.15	2.083225	1.804126	6.9092757	3.6082515
0.20	2.083325	1.804212	6.9096073	3.6084247
0.25	2.084175	1.804948	6.9124265	3.609897

The morphological study of all the compositions was done by SEM. Micrographs of all Gd doped nickel ferrite compositions are shown in Figure 5, Numerous voids and pores are visible in non-uniform agglomerated fragments [15]. It was observed that every grain was dispersed randomly and had non-uniform sizes [16]. The average grain size was found increased with Gd+3 composition and it was observed in the range of 140.5-176.2 nm, tabulated in Table 1.

Table 4. Variation of bond angles between cations and cation-anion situated in NiFe$_{2-x}$Gd$_x$O$_4$ (x=0.00, 0.05, 0.10, 0.15, 0.20 & 0.25) ferrite nano-particles annealed at 700℃

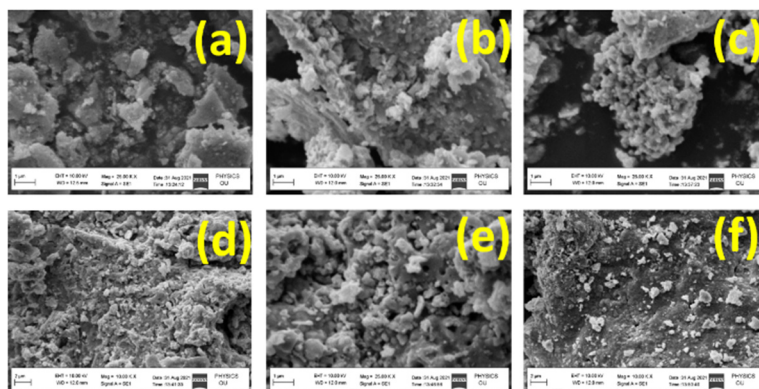| Gd Composition	θ₁	θ₂	θ₃	θ₄	θ₅
0.0	125.2644	128.7162	91.4562	125.2644	88.4764
0.05	125.2662	128.7421	91.51876	125.6989	88.48011
0.10	125.2714	128.7622	91.51945	126.0281	88.4827
0.15	125.2732	128.7713	91.56347	126.2492	88.48441
0.20	125.2754	128.7784	91.58002	126.3602	88.48526
0.25	125.2734	128.7862	91.58176	126.6956	88.48781

Figure 5. SEM images of NiFe$_{2-x}$Gd$_x$O$_4$ (x = 0.00, 0.05, 0.10, 0.15, 0.20 & 0.25) ferrite nano-particles annealed at 700℃

At room temperature, the magnetic properties of NiFe$_{2-x}$Gd$_x$O$_4$ (x = 0.00, 0.010, 0.15, 0.20 & 0.25) ferrite nano-particles were examined using a VSM. The synthesis method, grain size, cation doping, cation re-distribution, and other factors are major determinants of the magnetic properties of ferrite nano-particles [34]. Ferrite nano-particles' magnetic properties are mostly influenced by the Fe^{+3}-Fe^{+3} interaction and the spin coupling of their third-dimensional electrons. When Gd^{+3} enters the Fe lattice, according to the cation distribution, the Gd^{+3}-Fe^{+3} interaction happens with 3d-4f electrons spin coupling, and hence Gd^{+3} ions will replace Fe^{+3} ions in octahedral [B] site. Figure 6 illustrates the hysteresis of NiFe$_{2-x}$Gd$_x$O$_4$ (x = 0.00, 0.05, 0.10, 0.15, 0.20 & 0.25) ferrite nano-particles annealed at 700℃. The derived parameters such as saturation magnetization, remanent magnetization and coercivity are tabulated in Table 5.
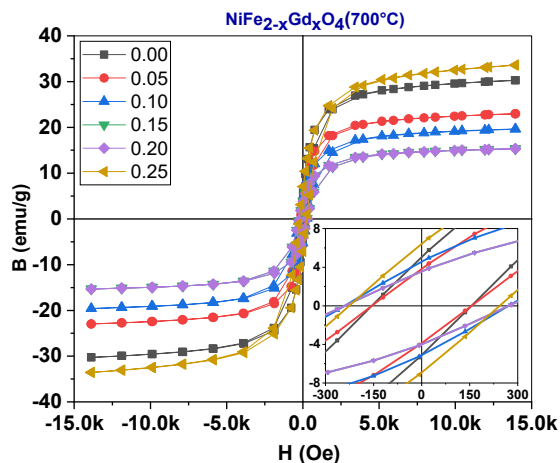

Figure 6. Hysteresis loops of NiFe$_{2-x}$Gd$_x$O$_4$ (x = 0.00, 0.05, 0.10, 0.15, 0.20 & 0.25) ferrite nano-particles annealed at 700℃

Table 5. Coercivity H$_C$ (Oe), residual magnetization M$_r$ (emu/g) and saturation magnetization M$_s$ (emu/g) of NiFe$_{2-x}$Gd$_x$O$_4$ (x = 0.00, 0.05, 0.10, 0.15, 0.20 & 0.25) ferrite nano-particles annealed at 700 ℃

Gd Composition	H$_c$ (Oe)	M$_r$(emu/g)	M$_s$(emu/g)
0.0	154	5.07	30.28
0.05	156	3.82	27.95
0.10	257	4.54	19.73
0.15	261	3.65	15.35
0.20	261	3.65	15.35
0.25	233	6.52	34.40

In general, Gd^{+3} ions have a magnetic moment of 7.9 BM whereas Fe^{+3} ions have magnetic moment 5 BM. Observing the Gd^{+3} and Fe^{+3} ions magnetic moments, the magnetization for all the compositions was supposed to increase Gd^{+3} composition in nickel ferrites. But it is clearly observed from Table-5 that M_s values and M_r values were decreased from 30.28 to 15.35 emu/g and 5.07 to 3.65 emu/g respectively. The coercivity was increased from 154 Oe to 261Oe and the magnetization change may be due to Gd^{+3}-Fe^{+3} interactions. Figure-7 illustrate the variation of coercivity (H_c) and saturation magnetization (M_s) for $NiFe_{2-x}Gd_xO_4$ (x = 0.00, 0.05, 0.10, 0.15, 0.20 & 0.25) ferrite nano-particles annealed at 700°C.
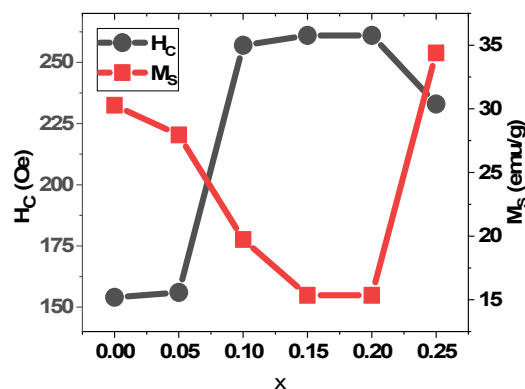

Figure 7. Variation of coercivity (H_C) and saturation magnetization (M_S) for $NiFe_{2-x}Gd_xO_4$ (x = 0.00, 0.05, 0.10, 0.15, 0.20 & 0.25) ferrite nano-particles annealed at 700°C

The strength of the spin-orbital coupling in ferrite materials limits their magnetic anisotropy. Presence of larger magnetic anisotropy in the ferrites results in the larger coercivity. Doping of Gd^{+3} ions in the nickel ferrites has resulted in the increase of coercivity which makes these ferrite compositions magnetically hard. Similar kind of results were observed for Tb^{+3} doped cobalt ferrites [35-36]. Presence of Gd^{+3} ions weaken the super-exchange interactions in nickel ferrites [37-38].

CONCLUSION

Sol gel auto-combustion was used to create $NiFe_{2-x}Gd_xO_4$ (x = 0.00, 0.010, 0.15, 0.20 & 0.25), ferrite nano-particles that were then annealed for eight hours at 700°C. The increased ionic radii of rare earth ions (Gd^{+3}) are responsible for the structural parameters, such as crystallite size and lattice parameter, which increased from 21.0288 to 27.04125 nm and 8.3325 to 8.3367Å, respectively, with Gd^{+3} composition. Estimates of the tetrahedral, octahedral, and bond-angles also demonstrated significant variation with the Gd^{+3} composition. The average grain size, which ranged from 140.5 to 176.2 nm, was found to increase with Gd composition. The composition of Gd resulted in a decrease in both saturation and residual magnetization. Gd content increases the coercivity and gives ferrite nano-particles their magnetic hardness.

ORCID

K. Vijaya Kumar, https://orcid.org/0000-0001-6160-8632; B. Purna Chandra Rao, https://orcid.org/0000-0001-7266-3338

REFERENCES
[1]   X. Li, J. Wei, K.E. Aifantis, Y. Fun, Q. Feng, F.-Z. Cui, and F. Watari, Journal of Biomedical Materials Research Part A, **104**(5), 1285 (2016). http://dx.doi.org/10.1002/jbm.a.35654
[2]   K.K. Kefeni, T.A. Msagati, T.T. Nkambule, and B.B. Mamba, Mater. Sci. Eng. C: Mater. Biol. Appl. **107**, 110314 (2020). https://doi.org/10.1016/j.msec.2019.110314
[3]   K.K. Kefeni, and B.B. Mamba, Sustainable Materials and Technologies, **23**, e00140 (2020). https://doi.org/10.1016/j.susmat.2019.e00140
[4]   M.I. Hussain, M. Xia, X.N. Ren, K. Akhtar, A. Nawaz, S.K. Sharma, and Y. Javed, in: *Magnetic Nanoheterostructures*, (Springer, Cham, 2020), pp. 243-265.
[5]   P.B. Kharat, B.S. Sandeep, P.K. Pankaj, and K.M. Jadhav, ACS omega, **5**(36), 23378 (2020). https://doi.org/10.1021/acsomega.0c03332
[6]   L.B. Tahar, M. Artus, S. Ammar, L.S. Smiri, F. Herbst, M.-J. Vaulay, V. Richard, et al., J. Magn. Magn. Mater. **320**, 3242 (2008). https://doi.org/10.1016/j.jmmm.2008.06.031
[7]   M.M. Rashad, R.M. Mohamed, and H. El-Shall, J. Mat. Proc. Tech. **198**(1–3), 139146 (2008). https://doi.org/10.1016/j.jmatprotec.2007.07.012
[8]   S.B. Narang, and K. Pubby, Journal of Magnetism and Magnetic Materials, **519**, 167163 (2020), https://doi.org/10.1016/j.jmmm.2020.167163
[9]   K.V. Kumar, Advances in Materials Physics and Chemistry, **12**(3), 33 (2022). https://doi.org/10.4236/ampc.2022.123003
[10] V.A. Bharati, S.R. Patade, S. Bajaj, R. Parlikar, A.P. Keche, and V.V. Sondur, Journal of Physics: Conference Series, **1644**, (1), 0120005 (2020). https://doi.org/10.1088/17426596/1644/1/012005
[11] N. Soltani, A.B. Syuhada, W.M.M. Yunus, E. Saion, and A. Bahrami, Solid State Comm. **192**, 15 (2014). http://dx.doi.org/10.1016/j.ssc.2014.05.002
[12] K.V. Kumar, R. Sridhar, and D. Ravinder, International Journal of Nano-particle Research, **2**(6), (2018). https://doi.org/10.28933/ijnr-2018-01-0302
[13] V.S. Puli, S. Adireddy, and C.V. Ramana, J. Alloys and Comp. **644**, 470 (2015). http://dx.doi.org/10.1016%2Fj.jallcom.2015.05.031

[14]   M. Humayun, H. Ullah, M. Usman, A. Habibi-Yangjeh, A.A. Tahir, C. Wang, and W. Luo, Journal of Energy Chemistry, **66**, 314 (2022). https://doi.org/10.1016/j.jechem.2021.08.023

[15]   J. Jiang, L. Li, F. Xu, and Y. Xie, Materials Science and Engineering: B, **137**(1-3), 166 (2007). http://dx.doi.org/10.1016/j.mseb.2006.11.014

[16]   J. Jing, L. Liangchao, and X. Feng, Journal of Rare Earths, **25**(1), 79 (2007). https://doi.org/10.1016/S1002-0721(07)60049-0

[17]   N.C. Sena, T.J. Castro, V.K. Garg, A.C. Oliveira, P.C. Morais, S.W. da Silva, **43**(5), 4042 (2017). https://doi.org/10.1016/j.ceramint.2016.11.155

[18]   Z.K. Heiba, M.B. Mohamed, L. Arda, and N. Dogan, Journal of Magnetism and Magnetic Materials, **391**, 195 (2015). https://doi.org/10.1016/j.jmmm.2015.05.003

[19]   K.R. Krishna, K.V. Kumar, and R. Dachepalli, Advances in Materials Physics and Chemistry, **2**, 185 (2012). http://dx.doi.org/10.4236/ampc.2012.23028

[20]   K.V. Kumar, and S.D. Bhavani, Science of Sintering, **54**(4), 457 (2022). https://doi.org/10.2298/SOS2204457K

[21]   A.T. Raghavender, N. Biliškov, and Z. Skoko, Materials Letters, **65**(4), 677 (2011). https://doi.org/10.1016/j.matlet.2010.11.071

[22]   L.J. Berchmans, R.K. Selvan, and C.O. Augustin, Materials Letters, **58**, 1928 (2004). http://dx.doi.org/10.1016/j.matlet.2003.12.008

[23]   Z. Yue, J. Zhou, L. Li, X. Wang, and Z. Gui, Materials Science and Engineering: B, **86**, 64 (2001). https://doi.org/10.1016/S0921-5107(01)00660-2

[24]   V.K. Katrapally, and S.D. Bhavani, Phase Transitions, **95**(11), 770 (2022). https://doi.org/10.1080/01411594.2022.2117622

[25]   [25] S.D. Bhavani, A.T. Raghavender, K.V. Kumar, and B.P.C. Rao, Eur. Chem. Bull. **12**(Special Issue 4), 10479 2023. https://doi.org/10.31838/ecb/2023.12.si4.0572023.22/04/202

[26]   V. Patil, S.E. Shirsath, S. More, S. Shukla, and K. Jadhav, Journal of Alloys and Compounds, **488**, 199 (2009). https://doi.org/10.1016/j.jallcom.2009.08.078

[27]   M. Kumari, and M.C. Bhatnagar, AIP Conference Proceedings, **2220**(1), 110042 (2020). http://dx.doi.org/10.1063/5.0002231

[28]   M.A. Yousuf, M.M. Baig, N.F. Al-Khali, M.A. Khan, M.F. Aly Aboud, I. Shakir, and M.F. Warsi, Ceram. Int. **45**, 10936 (2019). http://dx.doi.org/10.1016/j.ceramint.2019.02.174

[29]   T. Ahmad, S. Khatoon, K. Coolahan, and S. Lofland, Journal of Materials Research, **28**, 1245 (2013). https://doi.org/10.1557/jmr.2013.69

[30]   R.S. Yadav, I. Kuritka, J. Vilcakova, J. Havlica, L. Kalina, P. Urbanek, M. Machovsky, et al., Journal of Materials Science: Materials in Electronics, **29**, 15878 (2018). https://doi.org/10.1007/s10854-018-9674-z

[31]   P.P. Naik, R.B. Tangsali, S.S. Meena, and S.M. Yusuf, Mater. Chem. Phys. **191**, 215 (2017). https://doi.org/10.1016/j.matchemphys.2017.01.032

[32]   Z. Yan, and J. Luo, J. Alloys Compd. **695**, 1185 (2017). https://doi.org/10.1016/j.jallcom.2016.08.333

[33]   Z. Karimi, Y. Mohammadifar, H. Shokrollahi, Sh.Kh. Asl, Gh. Yousefi, and L. Karimi, J. Magn. Magn. Mater. **361**, 150 (2014). https://doi.org/10.1016/j.jmmm.2014.01.016

[34]   Z.K. Heiba, M.B. Mohamed, L. Arda, and N. Dogan, Journal of Magnetism and Magnetic Materials, **391**, 195 (2015). https://doi.org/10.1016/j.jmmm.2015.05.003

[35]   M.A. Dar, and D. Varshney, J. Magn. Magn. Mater. **436**, 101 (2017). https://doi.org/10.1016/j.jmmm.2017.04.046

[36]   T. Sodaee, A. Ghasemi, and E. Paimozd, Materials Physics and Mechanics, **17**, 11 (2013). https://www.ipme.ru/e-journals/MPM/no_11713/MPM117_03_sodaee.pdf

[37]   T. Sodaee, A. Ghasemi, E. Paimozd, A. Paesano, and A. Morisako, Journal of electronic materials, **42**, 2771 (2013). https://link.springer.com/article/10.1007/s11664-013-2656-2#citeas

[38]   K.K. Bamzai, G. Kour, B. Kaur, M. Arora, and R.P. Pant, Journal of magnetism and magnetic materials, **345**, 255 (2013). https://doi.org/10.1016/j.jmmm.2013.07.002

[39]   M.L. Kahn, and Z.J. Zhang, Applied Physics Letters, **78**(23), 3651 (2001). https://doi.org/10.1063/1.1377621

ВПЛИВ ВМІСТУ ГАДОЛІНІЮ НА МАГНІТНІ ТА СТРУКТУРНІ ХАРАКТЕРИСТИКИ НАНОЧАСТИНОК NFGO
Сара Дурга Бхавані[a,e], К. Віджая Кумар[b]*, А.Т. Рагхавендер[c], Дж. Арут Челвейн[d], Б. Пурна Чандра Рао[e]*
[a] Факультет хімії, державний коледж Раджендранагар, округ Рангаредді - 501218, Телангана, Індія
[b] Факультет фізики, JNTUH Університетський інженерний коледж Джагтіал, Начупаллі (Кондагату),
Округ Джагтіал 505501, Телангана, Індія
[c] Факультет фізики, Міжнародна школа технологій і наук для жінок, Раджамахендраварам,
Східний Годаварі -533 294, Андхра-Прадеш, Індія
[d] Магнітна група, Лабораторія оборонних металургійних досліджень, Канчанбаг, Хайдарабад-500058, Телангана, Індія
[e] Департамент хімії, Інститут технології та менеджменту Ганді, Хайдарабад-502 329, Телангана, Індія

Для створення наночастинок фериту нікелю, легованого гадолінієм, які мають хімічний склад NiFe$_{2-x}$Gd$_x$O$_4$ (x = 0,00, 0,010, 0,15, 0,20 і 0,25) було використано золь-гель автоспалювання. Дослідження було зосереджено на тому, як склад Gd+3 вплинув на магнітні властивості та структурні параметри. Магнітні властивості досліджували методом VSM, структурні властивості визначали методами XRD та SEM. XRD-графіки підтвердили встановлення шпінельної феритової фази. Зі збільшенням складу Gd розмір кристалітів і параметр гратки збільшилися з 21,0288 до 27,04125 нм і 8,3325 до 8,3367Å відповідно. Було також очевидно, як склад Gd+3 вплинув на оцінку зв'язкових кутів і довжин у тетраедричних і октаедричних структурах. Мікрофотографії SEM показали, що всі зерна мали невелику кількість агломерації і що всі синтезовані композиції були однорідними. Встановлено, що діапазон 140,5–176,2 нм є середнім розміром зерна. Використовуючи VSM при 300K, були обчислені такі магнітні параметри, як коерцитивна сила, залишкова намагніченість і намагніченість насичення. Поки склад не становив 0,20, намагніченість насичення та залишкова намагніченість падали з 30,28 emu/g до 15,35 emu/g і з 5,07 emu/g до 3,65 emu/g відповідно. Після цього вони зросли до 34,40 emu/g і 6,52 emu/g відповідно. До складу 0,20 коерцитивна сила була підвищена з 154 до 261 Oe; після цього його знизили до 233 E.
Ключові слова: *наночастинки фериту нікелю, леговані гадолінієм; золь-гель автозгоряння; XRD; SEM і магнітні властивості*